



Published in final edited form as:

Nat Cell Biol. 2009 November ; 11(11): 1383–1386. doi:10.1038/ncb1985.

DNA damage signalling prevents deleterious telomere addition at DNA breaks

Svetlana Makovets^{1,2} and Elizabeth H. Blackburn^{1,3}

¹ Department of Biochemistry and Biophysics, University of California, San Francisco, California 94143, USA

² Wellcome Trust Centre for Cell Biology, Institute of Cell Biology, University of Edinburgh, Edinburgh, EH9 3JR, UK

Abstract

The response to DNA damage involves regulation of multiple essential processes to maximize the accuracy of DNA damage repair and cell survival¹. Telomerase has the potential to interfere with repair by inappropriately adding telomeres to DNA breaks. It was unknown whether cells modulate telomerase in response to DNA damage, to increase the accuracy of repair. Here we report that telomerase action is regulated as a part of the cellular response to a DNA double-strand break (DSB). Using yeast, we show that the major ATR/Mec1 DNA damage signalling pathway regulates telomerase action at DSBs. Upon DNA damage, *MEC1-RAD53-DUN1*-dependent phosphorylation of the telomerase inhibitor Pif1 occurs. Utilizing a separation of function *PIF1* mutation, we show that this phosphorylation is required for the Pif1-mediated telomerase inhibition that takes place specifically at DNA breaks, but not telomeres. Hence DNA damage signalling down-modulates telomerase action at a DNA break via Pif1 phosphorylation, thus preventing aberrant healing of broken DNA ends by telomerase. These findings uncover a novel regulatory mechanism that coordinates competing DNA end-processing activities and thereby promotes DNA repair accuracy and genome integrity.

Nuclear DNA damage such as a broken replication fork that resembles a double strand break (DSB) can occur under normal mitotic growth conditions - i.e. in the absence of drugs or irradiation². A DSB can activate DNA damage signalling from the sensor kinases ATR and/or ATM (Mec1 and Tel1, respectively, in budding yeast) to the effector kinases Chk1 and Chk2 (Chk1 and Rad53/Dun1 in yeast), inducing cell cycle arrest and DNA repair¹. Appropriate DNA repair processes at DNA breaks include homologous recombination or non-homologous end-joining. However, telomerase is active during the S/G2 phase of the cell cycle^{3,4} and therefore can interfere with DSB repair by adding aberrant telomeres to broken DNA ends^{5,6}. Such *de novo* telomere addition may lead to terminal chromosomal deletions, associated with human genetic disorders and cancer^{7,8}. Pif1 helicase negatively regulates telomerase at both telomeres and DNA breaks^{5,6}. Cells lacking Pif1 have both longer telomeres and elevated frequencies of *de novo* telomere addition to DSBs⁶.

Users may view, print, copy, download and text and data- mine the content in such documents, for the purposes of academic research, subject always to the full Conditions of use: http://www.nature.com/authors/editorial_policies/license.html#terms

³Correspondence should be addressed to E.H.B. (Elizabeth.Blackburn@ucsf.edu).

Inactivation of DNA damage signalling in *mec1*, *rad53*, and other DNA damage response mutants also increases *de novo* telomere addition at spontaneous DNA breaks^{2,5}, which is further elevated in the absence of *PIF1*⁵.

We tested whether Pif1 is subjected to regulation in response to DNA damage. *PIF1* mRNA is translated using two alternative ATG start codons (M1 and M40) into two polypeptides: translation from M1 targets the resultant molecules to mitochondria whereas proteins synthesized from M40 are transported into the nucleus⁹. To selectively manipulate the nuclear form of Pif1 (nPif1) we placed two mutant copies of the *PIF1* gene at the endogenous *PIF1* locus: *pif1-m2* (M40 mutated) was a source of mitochondrial Pif1 and *pif1-m1* could provide only nPif1. We tested the effect of various DNA damage stimuli on nPif1. Treatment with phleomycin (radiomimetic) or hydroxyurea (leading to stalled replication forks), or a single unrepairable chromosomal DSB (induced by the expression of the HO endonuclease from a galactose-inducible promoter), each decreased nPif1-4myc mobility in gel electrophoresis (Fig. 1a).

We confirmed that the DSB-dependent mobility shift of nPif1 was due to phosphorylation using CIP phosphatase, which eliminated the DNA damage-induced nPif1 gel mobility shift (Fig. 1b). Interestingly, CIP phosphatase converted nPif1 from both undamaged cells and cells with an induced DSB into species that migrated faster than untreated nPif1 from undamaged yeast (Fig. 1b: compare lanes 7 and 8 to lane 5, also see Fig. 1d below). Together, these findings suggest that nPif1 predominantly consists of a species with a basal level of phosphorylation under normal conditions, and that additional phosphorylation occurs in response to DNA damage.

To test if the DSB-induced phosphorylation of nPif1 depended on the DNA damage response pathway, we induced the DSB in a set of isogenic *sm11* strains with either a functional DNA damage signaling network or missing one of its kinases, Mec1, Rad53, or Dun1. The *sm11* background was necessary to suppress the known lethality of *mec1* or *rad53*¹⁰ and the S-phase defect in *dun1*¹¹. Deletion of either *MEC1* or *RAD53*, but not *DUN1*, largely abolished the nPif1 phosphorylation (Fig. 1c). Thus, nPif1 undergoes Mec1- and Rad53-dependent phosphorylation in response to a single DSB. In contrast to the DNA damage-induced phosphorylation, the basal phosphorylation of nPif1 did not require the components of the damage signalling pathway (Fig. 1d).

We next tested whether the *RAD53*-dependent phosphorylation of nPif1 induced under conditions of DNA damage is necessary for the previously shown localization of nPif1 to the sites of damage repair¹². The efficiency of nPif1 accumulation at a single unrepairable break (DSB) was independent of *RAD53* (Fig. S1). Hence, the physical recruitment of nPif1 to a DSB does not require nPif1 phosphorylation via Rad53.

In the absence of nPif1, cells have longer telomeres and telomerase heals DSBs inappropriately by adding a new telomere ~200 times more frequently than in *PIF1* cells⁶. We searched for a Pif1 locus, potentially a phosphorylation site, important for the telomerase-inhibitory action of Pif1 that specifically occurs during a DNA damage response, i.e. at DSBs. *S. cerevisiae* Pif1 contains two regions - helicase motifs I-IV and V-VI -

homologous to other helicases¹³. The rest of the Pif1 protein, i.e. the middle part between the motif-containing regions as well as the N- and the C-terminal portions, have no obvious homologies, and we tested their involvement in the regulation of Pif1 by DNA damage signalling (Fig. 2a). Protein phosphorylation prediction program NetPhos 2.0 (www.cbs.dtu.dk) was used to scan Pif1 for potential phosphorylation at serine and threonine residues. Those residues with a prediction value above 0.25 in either the N-terminal or in the middle regions were mutated to non-phosphorylatable alanines to generate *PIF1* alleles with multiple substitutions, *pif1-N-18A* and *pif1-M-11A* respectively (Fig. 2a). In the C-terminus, all serines and threonines from T763 to the end were replaced with alanines to generate *pif1-C-18A*.

The effect of these mutations on Pif1 function at telomeres and DSBs was assayed by telomere length analysis and a genetic test for *de novo* telomere addition respectively (Fig. 2a and Fig. S2). As expected^{5, 6}, in the absence of nPif1 (*pif1-m2* cells), telomere length increased and the frequency of 5-FOA^R colonies, an indirect readout for *de novo* telomere addition, increased about 10-fold. *Pif1-N-18A* had only partial Pif1 function, causing both longer telomeres and more 5-FOA^R survivors. Pif1-M-11A was functional at both telomeres and DSBs. In a striking contrast, *pif1-C-18A* resembled *pif1-m2* (nuclear null) at DSBs (Fig. S2c) while remaining fully functional at inhibiting telomerase at telomeres (Fig. S2a). With only the 14 C-terminal serines and threonines mutated, Pif1-C-14A (see Fig. 2a) remained proficient at DSBs (Fig. S2c, compare C-18A and C-14A). This result narrowed down the candidate Pif1 locus involved in the Pif1 function of inhibiting telomerase at DSBs to the TLSSAES locus mutated in C-18A but not in C-14A (Fig. 2a).

We replaced the serines and the threonine of just the TLSSAES locus either with unphosphorylatable alanines (*pif1-4A*), or with potentially phosphomimetic aspartic acids (*pif1-4D*). Neither mutation caused any telomere length change (Fig. 2b), suggesting that both Pif1-4D and Pif1-4A were competent in inhibiting telomerase at telomeres. In contrast, in the *de novo* telomere addition to an induced DSB, *pif1-4A*, but not *pif1-4D*, was the same as *pif1-m2* (Fig. 2c). To determine the DNA rearrangements resulting in the 5-FOA^R colonies in the *PIF1*, *pif1-m2*, and *pif1-4A* strains, we analyzed DNA from multiple independent 5-FOA^R clones by Southern hybridization (Fig. S3). Consistent with previous reports, the frequency of *de novo* telomere addition was high in the absence of nPif1: all 11 out of 11 *pif1-m2* 5-FOA^R isolates had a new telomere added at the site of DSB, whereas none of the 12 *PIF1* colonies showed *de novo* telomere addition. Of 16 5-FOA^R *pif1-4A* clones, 15/16 had undergone the *de novo* telomere addition event. Hence, Pif1-4A cannot repress telomerase at DSBs. This strikingly contrasts with the unimpaired telomerase-inhibitory action of Pif1-4A at telomeres (Fig. 2b).

Localization of nPif1-4myc and nPif1-4A-4myc to an HO-inducible break were measured by chromatin immunoprecipitation (ChIP). The enrichment for the nPif1-4A mutant protein was consistently higher than for nPif1 (Fig. 2d). Therefore, nPif1-4A cannot suppress *de novo* telomere addition at a DSB despite its efficient physical localization to the site.

We next tested for nPif1 phosphorylation at the TLSSAES locus. nPif1-4A still underwent a mobility shift grossly similar to nPif1-wt in response to a single DSB (data not shown),

Author Manuscript

Author Manuscript

Author Manuscript

Author Manuscript

suggesting nPif1 is phosphorylated in response to DNA damage on sites other than TLSSAES. Therefore, to address phosphorylation specifically at the TLSSAES locus, we raised a phospho-specific polyclonal antibody corresponding to its inferred phosphorylated status in yeast cells. First, to determine which S/T at the cluster are likely to be phosphorylated *in vivo*, a set of 15 *pif1* mutants representing all possible combinations of T→A and S→A substitutions were tested for *de novo* telomere addition as described above (Fig. 2c). No single amino acid substitution noticeably affected the low frequency of 5-FOA^R colony formation characteristic of *PIF1* cells (Table S1). However, the double substitution Pif1(T763A S766A) resulted in a significant increase in the 5-FOA^R survivors, suggesting that the combination of phosphorylations on T763 and S766 could be important for telomerase regulation at DSBs. Therefore, we raised rabbit polyclonal antibodies, anti-P-Pif1, specifically against the phospho-peptide VIDFYL(pT)LS(pS)AE. Antibody specificity was confirmed by immunoprecipitating nPif1-4myc and nPif1-4A-4myc from cells without and with a single DSB. The antibody recognized nPif1-4myc from cells after DSB induction but not from uninduced cells, and its binding to Pif1 was significantly reduced by the *pif1-4A* mutation (Fig. 2e). These results indicated that the antibody was specific to the TLSSAES locus, and to its state induced by DSBs. CIP phosphatase treatment of immunoprecipitated proteins abolished the ability of the antibody to recognize nPif1-4myc from cells with DNA damage, showing that the phosphorylation of TLSSAES was required for the antibody to bind Pif1. Therefore, we conclude that nPif1 is phosphorylated at T763 and S766 in response to DSBs. Furthermore, this DSB-induced phosphorylation was also dependent on the key components of the DNA damage signalling pathway Mec1, Rad53, and Dun1 (Fig. 2f). Interestingly, the TLSSAES locus shares sequence similarity with the Sml1 regulatory locus SASSLEM which is also a subject of Dun1-dependent phosphorylation¹⁴. Therefore, we established a direct link between the DNA damage signalling and the Pif1-dependent regulation of telomerase at DSBs. Although *pif1-m2* did not show epistatic interactions with mutations inactivating the signalling pathway⁵, this could be due to the pleiotropic roles of the DNA damage signalling kinases.

Because DSB induction holds up yeast cells in G2, we tested whether TLSSAES phosphorylation was simply a characteristic of the G2 stage of the cell cycle. However, nocodazole alone caused no TLSSAES phosphorylation (Fig. 2g, lanes 5–6), whereas induction of the DSB in the nocodazole-arrested cells resulted in phosphorylation of the TLSSAES locus (Fig. 2g, lanes 7–8). Therefore, Pif1 phosphorylation on the TLSSAES locus is not attributable simply to the G2 stage of the cell cycle, but rather, requires activation of DNA damage signalling.

Like DNA breaks, stalled replication forks also activate DNA damage signalling¹⁵. However, the TLSSAES locus was not phosphorylated in response to hydroxyurea (Fig. 2h). Thus, the regulation of nPif1 through TLSSAES may be specific to a situation where telomerase has a strong potential of interfering with the DNA repair machinery, namely DSBs.

The DNA damage response preserves genome stability and cell survival under conditions of DNA damage stress. Our findings uncover a novel mechanism by which DNA damage signalling ensures telomerase action is not deployed inappropriately at a DNA damage site.

The key target of this *MEC1-RAD53-DUN1*-dependent signalling pathway is the telomerase-inhibitory helicase nPif1. This mechanism acts to rein in deleterious DSB-specific telomerase action and thus preserves genomic integrity. Components of this DNA damage signalling pathway as well as Pif1 and telomerase are conserved from yeast to mammals and interaction between mouse Pif1 and telomerase has been reported¹⁶. Hence similar regulation of Pif1 by the DNA damage signalling network may be evolutionarily conserved in eukaryotes.

Supplementary Material

Refer to Web version on PubMed Central for supplementary material.

Acknowledgments

We thank members of the Blackburn and Harrington labs for encouraging discussions and useful ideas. We also thank Carol Anderson for pEHB13045 and Heidrun Interthal and Noreen E. Murray for critical reading of the manuscript and helpful suggestions. We thank the laboratory of Lea A. Harrington for support of S.M. since February 2008 (with funds provided by the School of Biological Sciences, University of Edinburgh, and Wellcome Trust Programme Grant 84637 to Lea A. Harrington). This work was supported by NIH grant GM26259 (to E.H.B.).

References

1. Harper JW, Elledge SJ. *Mol Cell*. 2007; 28:739–745. [PubMed: 18082599]
2. Myung K, Datta A, Kolodner RD. *Cell*. 2001; 104:397–408. [PubMed: 11239397]
3. Diede SJ, Gottschling DE. *Cell*. 1999; 99:723–733. [PubMed: 10619426]
4. Marcand S, Brevet V, Mann C, Gilson E. *Curr Biol*. 2000; 10:487–490. [PubMed: 10801419]
5. Myung K, Chen C, Kolodner RD. *Nature*. 2001; 411:1073–1076. [PubMed: 11429610]
6. Schulz VP, Zakian VA. *Cell*. 1994; 76:145–155. [PubMed: 8287473]
7. Lasko D, Cavenee W, Nordenskjold M. *Annu Rev Genet*. 1991; 25:281–314. [PubMed: 1687498]
8. Wilkie AO, Lamb J, Harris PC, Finney RD, Higgs DR. *Nature*. 1990; 346:868–871. [PubMed: 1975428]
9. Lahaye A, Stahl H, Thines-Sempoux D, Foury F, Embo J. *Embo J*. 1991; 10:997–1007. [PubMed: 1849081]
10. Zhao X, Muller EG, Rothstein R. *Mol Cell*. 1998; 2:329–340. [PubMed: 9774971]
11. Zhao X, Rothstein R. *Proc Natl Acad Sci U S A*. 2002; 99:3746–3751. [PubMed: 11904430]
12. Wagner M, Price G, Rothstein R. *Genetics*. 2006; 174:555–573. Epub 2006 Jul 2002. [PubMed: 16816432]
13. Bessler JB, Torredagger JZ, Zakian VA. *Trends Cell Biol*. 2001; 11:60–65. [PubMed: 11166213]
14. Uchiki T, Dice LT, Hettich RL, Dealwis C. *J Biol Chem*. 2004; 279:11293–11303. [PubMed: 14684746]
15. Sun Z, Fay DS, Marini F, Foiani M, Stern DF. *Genes Dev*. 1996; 10:395–406. [PubMed: 8600024]
16. Snow BE. et al *Mol Cell Biol*. 2007; 27:1017–1026.

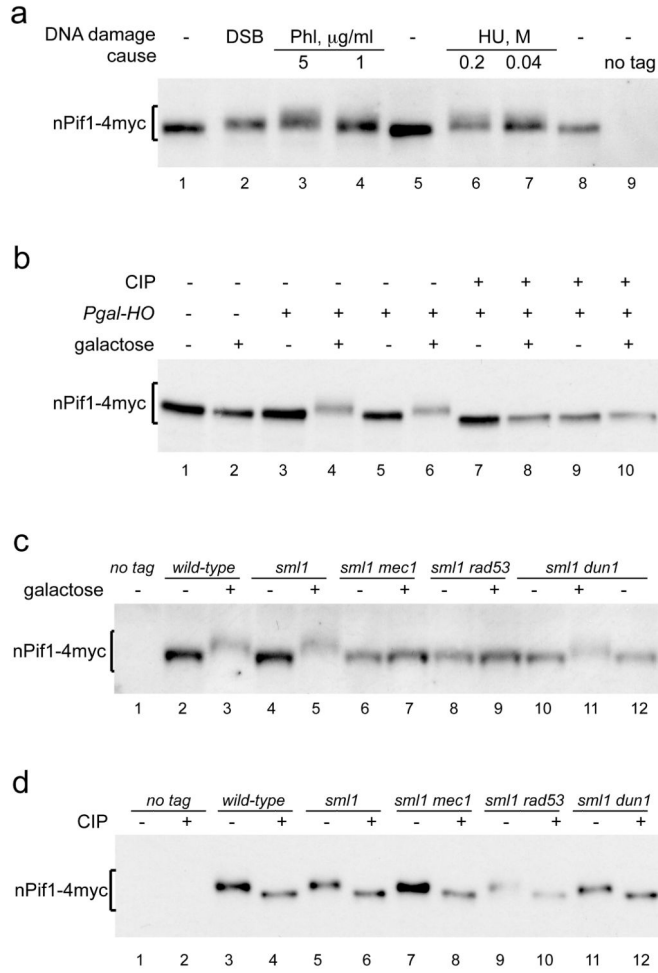


Figure 1. nPif1 is phosphorylated in response to DNA damage in a *MEC1-RAD53* dependent manner. In all the panels (**a–d**), gel mobility of nPif1-4myc either from total protein extracts (panels **a** and **c**) or after immunoprecipitation and CIP phosphatase treatments (panels **b** and **d**) is analysed by western blotting using an α -myc antibody. **a**, Analysis of nPif1 gel mobility in response to different DNA damage stimuli. Cells were grown to mid-log phase in rich medium with raffinose. DSBs were induced by addition of galactose (see Methods Summary). Alternatively, either phleomycin (Phl) or hydroxyurea (HU) were added to the concentrations indicated. After 2 h cells were harvested for protein analysis. **b**, nPif1 is phosphorylated in response to a single DSB induced by the expression of the HO endonuclease from a galactose-inducible promoter. **c**, nPif1 phosphorylation in response to a single DSB requires *MEC1* and *RAD53*. **d**, Basal phosphorylation of nPif1 is independent of the DNA damage signalling kinases.

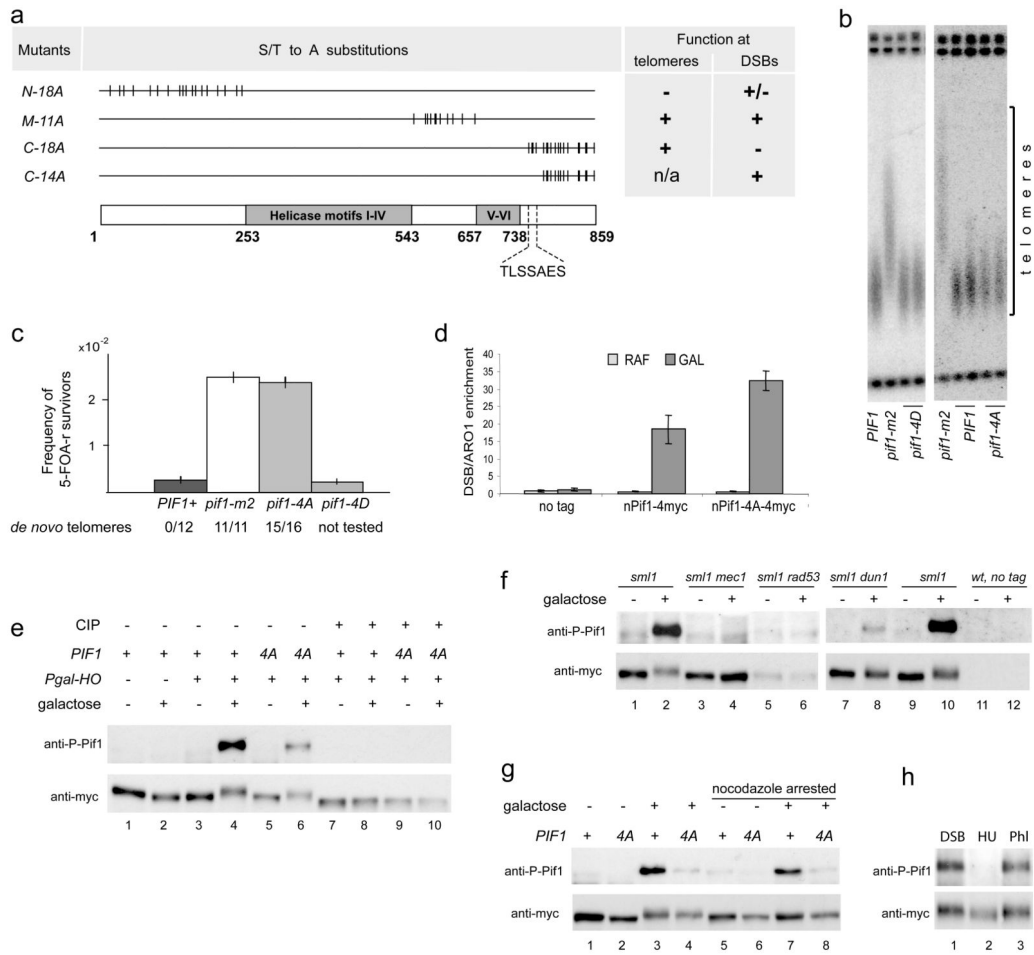


Figure 2. *pif1-4A* is a separation of function phospho-site mutant, defective in telomerase inhibition specifically at DSBs and not telomeres. **a**, Mutagenesis based scanning of nPif1 for potential phosphorylation loci involved in its function during DNA damage response. Schematic of the multiple S/T→A substitutions constructed in different nPif1 regions (See Methods for details) and summary of mutant phenotypes (on the right, data presented in Fig. S2). **b**, Telomere length analysis in *PIF1*, *pif1-m2*, *pif1-4D*, and *pif1-4A* cells. **c**, Frequency of 5-FOA^R colony formation in *PIF1*, *pif1-m2*, *pif1-4A*, and *pif1-4D* upon DSB induction. Error bars represent average ± s.d. from four independent measurements for each strain, except *pif1-4D* (three measurements). Note that the majority of 5-FOA^R colonies from *PIF1* cells do not represent *de novo* telomere addition events whereas the majority of the same class of clones from *pif1-m2* and *pif1-4A* do (see the numbers under the graph and Fig. S3). **d**, Analysis of nPif1-4myc and nPif1-4A-4myc localization to a galactose inducible DSB by chromatin immunoprecipitation. Error bars show average ± s.d. from four independent experiments. **e**, TLSSAES is phosphorylated in response to a single DSB. Note that the anti-P-Pif1 antibody has weak cross-reactivity with another DNA damage induced phosphorylation site on Pif1 as seen in lane 6 (*pif1-4A* in galactose). However, this does not affect the conclusiveness of the data as there is a significant signal difference between *PIF1*

and *pif1-4A* (compare lanes 4 and 6). The same applies to panels **f** and **g**. **f**, TLSSAES phosphorylation in response to a single DSB requires *MEC1*, *RAD53*, and *DUN1*. **g**, TLSSAES is phosphorylated in response to DSBs but not in response to nocodazole-induced G2 arrest. **h**, TLSSAES is phosphorylated in response to DSBs (DSB and Phleomycin, Phl) but not stalled replication forks (hydroxyurea, HU). DNA damage was induced as in Fig. 1. In the panels **e-h**, samples of immunoprecipitated nPif1-4myc were analyzed by western blotting using an affinity purified rabbit polyclonal antibody raised against VIDFYL(pT)LS(pS)AE (anti-P-Pif1, upper blot on each panel) and then re-probed with anti-myc antibody (lower blot).